International Journal of Chemical, Material and Environmental Research 2018, 5 (1): 137-147

Research article

IJCMER
www.ijcmer.org

INTERNATIONAL JOURNAL OF CHEMICAL, MATERIAL AND ENVIRONMENTAL RESEARCH

An International Open Free Access, Peer Reviewed Research Journal

ISSN 2410-5945
2018, Vol. 5, No. 1:
pg. 137-147

Free Convective Heat and Mass Transfer – An Applied Mathematical Approach to a Qualitative Engineering Research

Anselm O. Oyem

Department of Mathematical Sciences, Federal University Lokoja, Kogi State, PMB 1154, Nigeria

(Received: December 05, 2017; Accepted: February 13, 2018)

Abstract

In this paper, a steady two-dimensional incompressible free convective fluid flow with slip and thermal conductivity variation was used to explain the mathematical concept of heat and mass transfer and its application in qualitative engineering research problems. Using similarity variables, the governing partial differential equations are transformed into a set of coupled non-linear ordinary differential equations and solved numerically using shooting method and Runge-Kutta fourth order scheme. Some of the thermo-physical behaviours associated with the problem are considered and graphical results are presented showing the effects of the governing parameters on dimensionless velocity, temperature and concentration. The numerical results on Nusselt number, shear stress and Sherwood number are also presented. The results indicate that there are significant effects of the controlling parameters on the flow field.

Keywords: Free convection, heat and mass transfer, qualitative engineering, ode

1. Introduction

According to Harvard School of Engineering and Applied Sciences, applied mathematics focuses on the creation and study of mathematical and computational tools broadly applicable in sciences and engineering, and on their use in solving challenging problems in these and related fields. Furthermore, such applications occur in many field of human endeavour like the probed limit of democracy as an institute by calculating the probabilities that decisions cannot be reached on purely rational terms, reduction in the green-house emission, creating more quantitative basis for modern information technologies [1,2].

Free convective heat and mass transfer is an applied process involved when energy and mass are transferred from one region to another due to temperature differences. It is a computational means to many scientific and engineering researches as many scientific problems that were previously inaccessible have received tremendous progress. From literature, there has been an increasing need for the continuous study of the behaviour on free convective flow driven by the influence of temperature differences, magnetic field, electromagnetic field, heat and mass transfer, radiation, due to its wide range of growing needs and applications. In the field of agriculture, science and technology, geophysics, astrophysics, geological formations and thermal recovery of oil, assessment of aquifers, geothermal reservoirs and underground nuclear waste storage site, metallurgy and aerodynamic extrusion of plastic sheets. It is applicable in engineering and petroleum industries such as petroleum engineering, chemical engineering, composite or ceramic engineering and heat exchanger, nuclear reac-

* Corresponding author:
onyekachukwu.oyem@fulokoja.edu.ng, anselmoyemfulokoja@gmail.com
Published online at www.ijcmer.org

tor and combustion; solar collectors, drying, dehydration operations in chemical and food processing plants, polymer production, thermal insulation, enhanced oil recovery. Also they are applicable in underground energy transport and cooling of nuclear reactor, heating and cooling chambers, fossil fuel combustion energy processes evaporation from large open water reservoirs, astrophysical flows, and solar power technology. Furthermore, space technology, cooling of cutting tools during a machining operation, electronic components in a computer. Similarly, in buildings, cooking, thermal control of a re-entering spacecraft, generation and condensation of steam in a thermal power plant [3, 4, 5, 6, 7]. Similarly, modeling of large structure amplitude, slender, flexible and cantilever beam carrying a lumped mass [14].

In this paper, a simple steady two-dimensional free convective heat and mass transfer flow problem of a viscous and incompressible fluid over a vertical plate with variable thermal conductivity will be considered and used to explain the mathematical concept behind qualitative engineering researches. It is very important to note that nothing in science and engineering can be done without considering heat and mass transfer thus; the governing partial differential equations will be transformed to a set of coupled nonlinear ordinary differential equations using similarity variables. The results obtained will be used to explain the concept of reducing radiation exposure emanating from indiscriminate masking of telecommunication stations and electricity distribution cables.

2. Mathematical Formulation of the Problem

A steady two-dimensional laminar free convective heat and mass transfer fluid flow of a viscous, incompressible fluid over a vertical plate with variable thermal conductivity is considered. The flow in the x-axis was taken along the vertical plate in the upward direction and the y-axis normal to the plate where T_w and C_w are temperature and concentration of the fluid at the plate and T_∞ and C_∞ the temperature and concentration outside the boundary layer. Under Boussinesq's approximation, the model equations are given as [3, 8];

$$\frac{\partial u}{\partial x}+\frac{\partial v}{\partial y}=0 \tag{1}$$

$$u\frac{\partial u}{\partial x}+v\frac{\partial u}{\partial y}=v\frac{\partial^2 u}{\partial y^2}+g\beta(T-T_\infty)+g\beta^*(\mathrm{C}-C_\infty)-\frac{\sigma\beta_0^2 u}{\rho} \tag{2}$$

$$u\frac{\partial T}{\partial x}+v\frac{\partial T}{\partial y}=\frac{1}{\rho c_p}\frac{\partial}{\partial y}\left(k(T)\frac{\partial T}{\partial y}\right)-\frac{1}{\rho c_p}\frac{\partial q_r}{\partial y}+\frac{Q_0}{\rho c_p}(T-T_\infty) \tag{3}$$

$$u\frac{\partial C}{\partial x}+v\frac{\partial C}{\partial y}=D\frac{\partial^2 C}{\partial y^2} \tag{4}$$

with boundary conditions

$$\begin{aligned} &u=0 \quad v=0 \quad T=T_w \quad C=C_w \quad \text{at} \quad y=0\\ &u\to 0 \quad T\to T_w \quad C\to C_w \quad \text{at} \quad y\to\infty \end{aligned} \tag{5}$$

where, u, v are the velocity components in x, y–directions respectively, ρ is density of the fluid, c_p the specific heat capacity at constant pressure, v is the kinematic viscosity, g is acceleration due to gravity, σ is electrical conductivity, T is temperature of the fluid, C is concentration of the fluid, β and β^* are thermal and concentration coefficients of volumetric expansion, β_0 is the magnetic field intensity, $\kappa(T)$ is variable thermal conductivity of the fluid, D is the coefficient of mass diffusivity, Q_0 is heat absorption coefficient and the radiative heat flux q_r.

From Equation 3, let the radiative heat flux q_r be described by Rosseland approximations and if the temperature differences within the flow are assumed to be sufficiently small so that T^4 may be expressed as a linear function of temperature T using Taylor's series and, assume that the fluid thermal conductivity κ vary as a linear function of temperature [9] then,

$$T^4\cong 4T_\infty^{\,3}T-3T_\infty^{\,4} \tag{6}$$

$$q_r=-\frac{16\sigma^* T_\infty^{\,3}}{3k^*}\left(\frac{\partial^2 T}{\partial y^2}\right) \tag{7}$$

$$\kappa(T) = \kappa^{*}\left[1+\delta^{*}(T-T_{\infty})\right] \quad 8$$

Introducing stream function ψ(*x*, *y*) and applying Equations 6-8 in Equations 1-5 with the following similarity variables,

$$\eta = y\sqrt{\frac{U_0}{2\nu x}} \qquad \psi = \sqrt{2x\nu U_0 f(\eta)} \qquad \theta(\eta) = \frac{T-T_{\infty}}{T_w - T_{\infty}} \quad 9$$

Equation 1 is satisfied and Equations 2-5 reduces to the following coupled nonlinear ordinary differential equations

$$\frac{d^3 f}{d\eta^3} + f\frac{d^2 f}{d\eta^2} + Gr\theta + Gm\phi - M\frac{df}{d\eta} = 0 \quad 10$$

$$\left(1+\gamma\theta+\frac{4}{3N}\right)\frac{d^2\theta}{d\eta^2} + Prf\frac{d\theta}{d\eta} + \gamma\left(\frac{d\theta}{d\eta}\right)^2 + PrQ\theta = 0 \quad 11$$

$$\frac{d^2\phi}{d\eta^2} + Scf\frac{d\phi}{d\eta} = 0 \quad 12$$

subject to the conditions

$$\eta = 0;\ \ f = 0 \qquad \frac{df}{d\eta} = 0 \qquad \theta = 1 \qquad \phi = 1 \quad 13$$

$$\eta \to \infty;\ \ \frac{df}{d\eta} \to 0 \qquad \theta \to 0 \qquad \phi \to 0$$

where prime denotes the differentiation with respect to η. It is noteworthy that the local parameters: local Grashof number (*Gr*), local mass Grashof number (*Gm*), local magnetic field parameter (*M*) and local heat generation/source parameter (*Q*) are functions of *x* in Equations 10-12 subject to conditions in Equation 13. The problem under consideration is a physical one hence; there is the need to confirm that the set of assumptions taken are right. Thus, their qualitative properties would be established by the existence and uniqueness of the solution and stability of solution via Lyapunov. This process can be achieved by first transforming the coupled nonlinear ordinary differential equations into a system of ordinary linear equations.

3. Numerical Procedures

The coupled nonlinear differential Equations 10-12 under the boundary layer conditions in Equation 13 are solved numerically by Runge-Kutta fourth order technique and shooting method. Effects of the prescribed parameters; *Gr*, *Gm*, *M*, Prandtl number (*Pr*), *Q*, Schmidt number (*Sc*), variable thermal conductivity (γ) and thermal radiation (*N*) on velocity, temperature and concentration profiles are presented in Figures 1-8. First, we obtained a system of linear equations say; let

$$f = x_1,\ \ f' = x_2,\ \ f'' = x_3,\ \ \theta = x_4,\ \ \theta' = x_5,\ \ \phi = x_6,\ \ \phi' = x_7$$

then, Equations 10-13 are transformed to a system of first order differential equations

$$\begin{aligned}
x_1' &= x_2 \\
x_2' &= x_3 \\
x_3' &= Mx_2 - Grx_4 - Gmx_6 - x_1x_3 \\
x_4' &= x_5 \\
x_5' &= \left(\frac{3N}{3N(1+\gamma x_4)+4}\right)(-Prx_1x_5 - \gamma x_5^2 - PrQx_4) \\
x_6' &= x_7 \\
x_7' &= -Scx_1x_7
\end{aligned} \quad 14$$

subject to the following boundary initial conditions

$$x_1 = 0,\ \ x_2 = 0,\ \ x_3 = s_1,\ \ x_4 = 1,\ \ x_5 = s_2,\ \ x_6 = 1,\ \ x_7 = s_3 \quad 15$$

with the unspecified initial conditions s_1, s_2 and s_3. The numerical computations are simply implemented using MATLAB with fixed step-size of $\Delta\eta = 0.001$ chosen to satisfy the convergence criterion 10^{-6}. The skin friction coefficient $f''(0)$, Nusselt number $-\theta'(0)$ and mass transfer coefficient in terms of Sherwood number $-\phi'(0)$ were also worked out and their numerical values are presented in Table 1.

4. Results and Discussion

The effects of velocity, temperature and concentration profiles had been displayed in Figures 1-8. Skin-friction coefficient, Nusselt and Sherwood numbers were also computed for various values of the governing parameters: *N*, *Gr*, *Gm*, *Pr*, *M*, *Sc*, *Q*, and γ as presented in Table 1. It was observed from Table 1 that shear stress in terms of skin friction coefficient increases slightly as variable thermal conductivity, buoyancy parameter and thermal radiation parameter increases but decreases with increase in Schmidt number, Prandtl number and local magnetic field parameter. Also, a decrease in the local mass Grashof number and local heat source parameter led to a decrease in skin friction but as γ, *N*, *M*, *Sc* and *Q* increases, the rate of heat transfer decreases. Similarly, as Prandtl number, local Grashof and local mass Grashof number increases, the Nusselt number decreases respectively. However, it was also observed that the rate of mass transfer increases with increasing values of *M* and *Pr* but decreases as *Gr*, *Gm*, *N*, *Sc* and *Q* increases in value.

Table 1. Numerical Values of $f''(0)$, $-\theta'(0)$ and $-\phi'(0)$ for Various Values of the Governing Parameters for Equations 10–12

γ	*Pr*	*Gr*	*N*	*M*	*Gm*	*Sc*	*Q*	$f''(0)$	$-\theta'(0)$	$-\phi'(0)$
0.5	0.71	1.0	1.2	1.0	1.5	0.22	0.01	1.8199	0.2772	0.2810
1.0								1.8325	0.2525	0.2830
1.5								1.8434	0.2330	0.2848
2.0								1.8530	0.2173	0.2865
0.5	0.71	1.0	1.2	1.2	1.5	0.22	0.01	1.7358	0.2689	0.2729
	1.0							1.7073	0.3175	0.2669
	3.0							1.6078	0.5169	0.2515
	5.0							1.5608	0.6341	0.2467
0.5	0.72	1	0.10	2	1.2	0.32	0.01	1.2581	0.2965	0.2652
		3						2.2337	0.3705	0.3263
		5						3.1350	0.4213	0.3693
		7						3.9863	0.4609	0.4031
0.5	0.71	1.0	0.1	1.2	1.5	0.2	0.01	1.6898	0.3579	0.2503
			1.0					1.7390	0.2828	0.2597
			2.0					1.7693	0.2365	0.2665
			3.0					1.7881	0.2083	0.2709
0.5	0.72	1.0	0.10	2	2.0	0.21	0.1	1.7269	0.3045	0.2492
				4				1.3416	0.2302	0.2084
				6				1.1346	0.1790	0.1854
				8				1.0011	0.1402	0.1706
0.5	0.72	1.2	0.10	2	1.0	0.22	0.01	1.2715	0.3017	0.2211
					1.5			1.5431	0.3298	0.2403
					2.0			1.8100	0.3540	0.2573
					2.5			2.0724	0.3754	0.2726
0.5	0.71	1.2	0.10	1	1.5	0.22	0.1	1.8857	0.3342	0.2753
						0.32		1.8384	0.3210	0.3270
						0.42		1.8023	0.3107	0.3704
						0.52		1.7732	0.3024	0.4080
0.5	0.72	1	0.10	2	1.0	0.22	0.01	1.1677	0.2920	0.2153
							0.04	1.1725	0.2751	0.2162
							0.08	1.1793	0.2517	0.2174
							0.10	1.1829	0.2394	0.2181

The effect of variable thermal conductivity on velocity, temperature and concentration profiles are presented in Figures 1a-1c. It was observed from Figure 1a that as γ increases in value, velocity increases steeply to a peak along the plate and decreases gradually away from the plate towards the free stream. In Figure 1b, temperature profiles increases with increasing values of thermal conductivity variation parameter γ, while from Figure 1c, concentration profiles decreases with increased values of variable thermal conductivity.

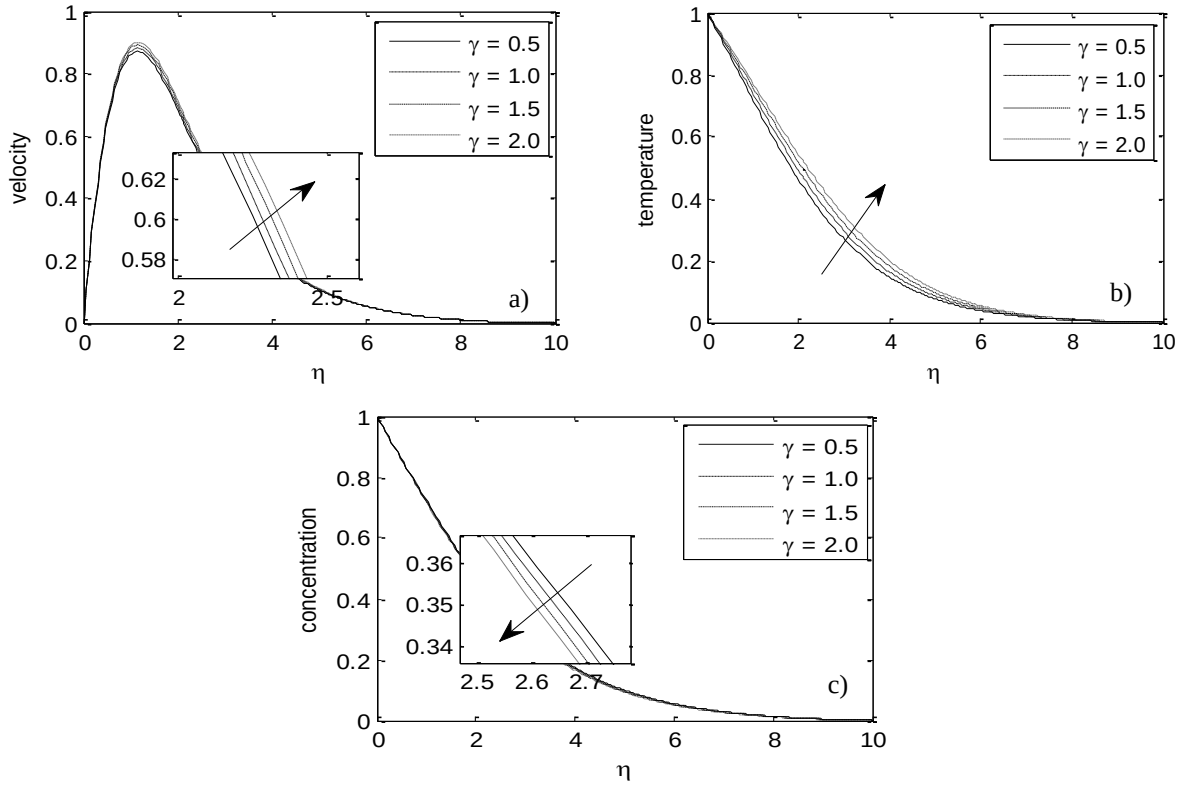

Figure 1. Velocity (a), Temperature (b) and Concentration (c) Profiles over a Vertical Plate for Various Values of γ

The effects of *Pr* on velocity, temperature and concentration profiles are displayed in Figures 2a, 2b and 2c respectively. Figure 2a showed that with an initial rise of *Pr* = 0.71,1.0, the flow velocity profiles gradually decreased away from the plate towards the free stream as *Pr* increases. In Figure 2b, temperature profiles decreases rapidly along the plate as *Pr* increases. It was interesting to note here that at *Pr* = 0.71,1.0, the flow pattern rose slightly in the thermal boundary layers near the plate but decreased sharply for *Pr* = 3.0 towards the plate [10].

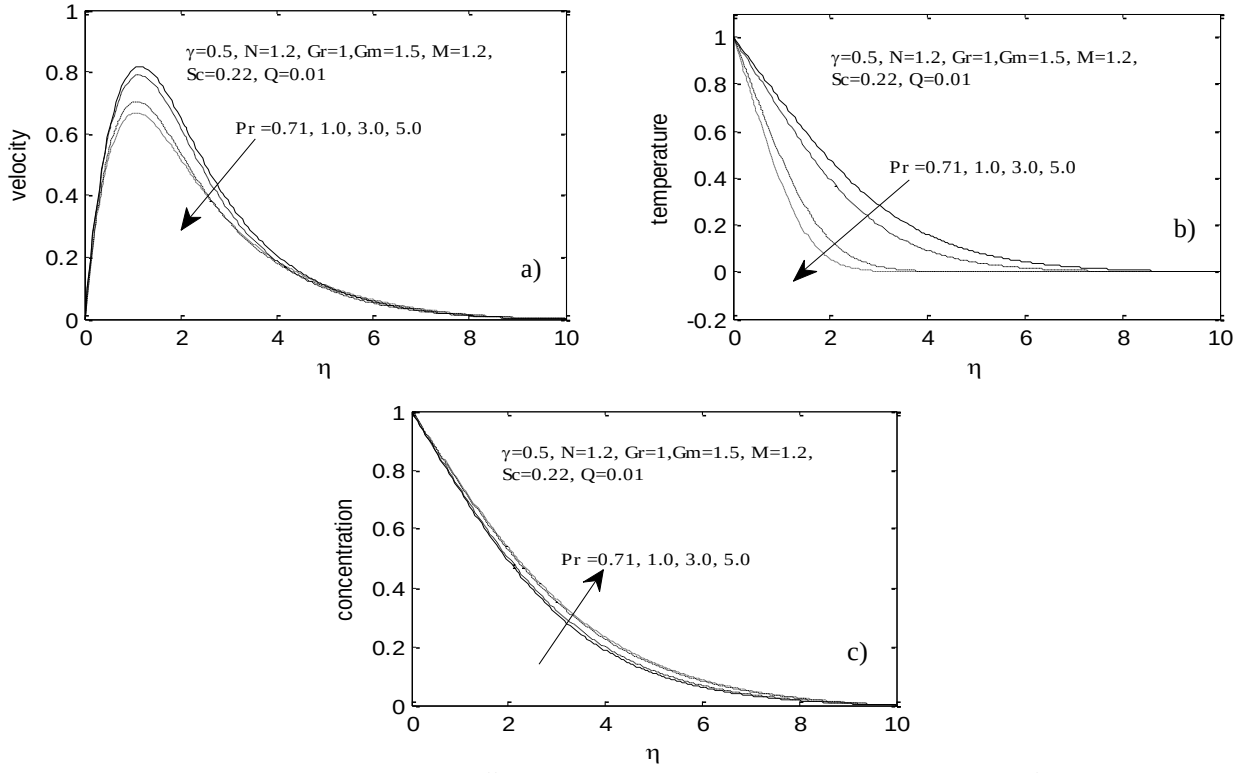

Figure 2. Prandtl Number (*Pr*) Effect on Velocity (a), Temperature (b) and Concentration (c) profiles

In Figure 2c, increase in *Pr* resulted in the increase in concentration profiles. It increased gradually away from the vertical plate towards the free stream. But a distinction was observed from the figure that for $Pr \geq 3.0$, the concentration profile increases slightly more away from the plate. Figures 3a–3c shows the variation of *Gr* on velocity, temperature and concentration profiles.

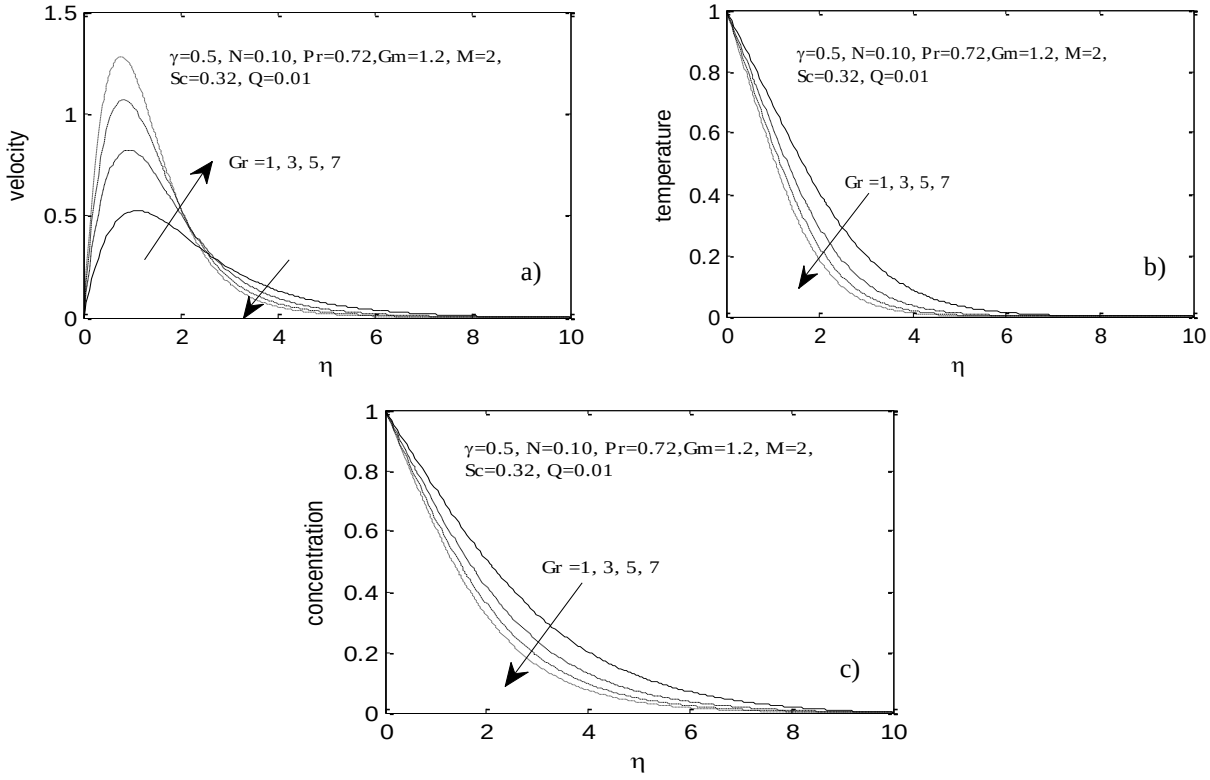

Figure 3. Local Grashof Number (*Gr*) Variation on Velocity (a), Temperature (b) and Concentration (c) Profiles

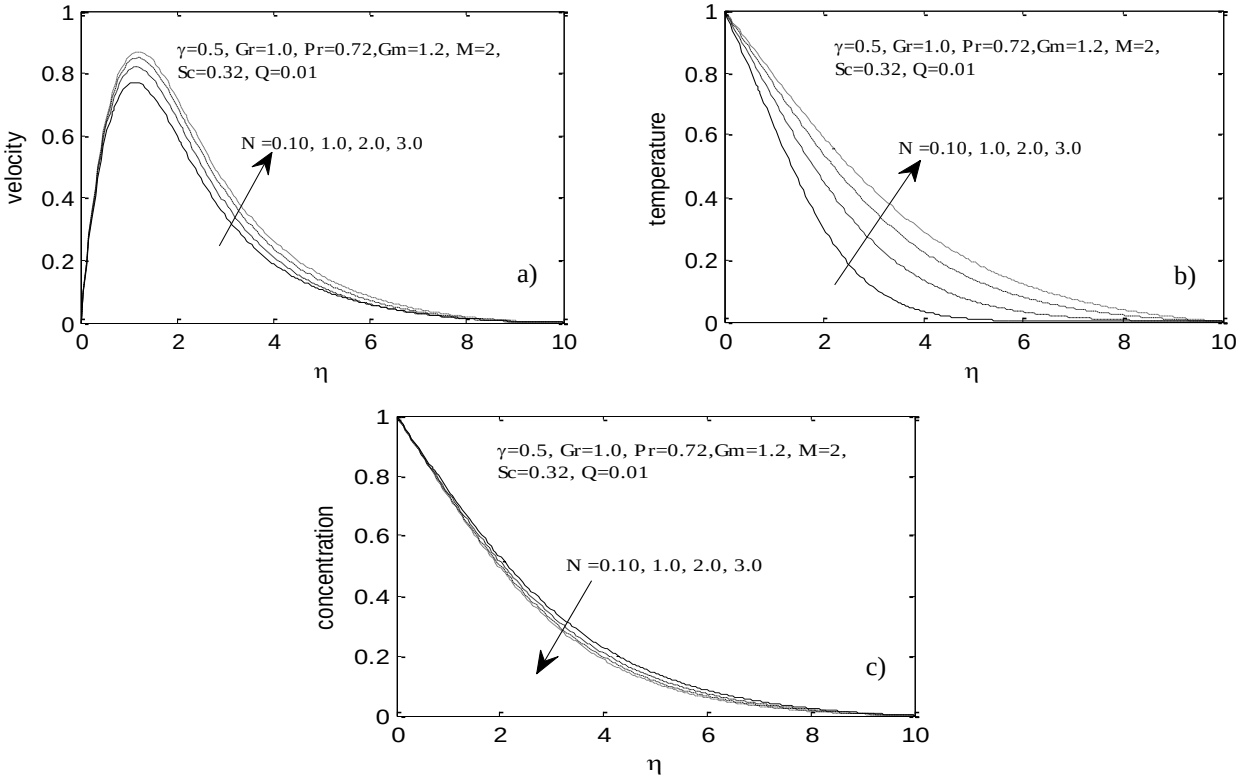

Figure 4. Velocity (a), Temperature (b) and Concentration (c) Profiles against η for Varying Values of *N*

From Figure 3a, it was observed that velocity profiles increases spontaneously initially near the vertical plate as *Gr* increases but a cross flow in the velocity was induced along the flow as velocity decreases away from the plate at a slower rate to the free stream with increasing values of *Gr*. Since *Gr*>0 corresponds to externally cooled plate, substantial increase in velocity distribution profiles were observed near the plate, thereby indicating greater cooling results in velocity increase and thermal boundary layer thickness. This situation revealed that buoyancy force accelerates the velocity field and no flow reversal occurs to prevent separation [10,11]. The effect of *Gr* on temperature and concentration profiles are presented in Figures 3b and 3c. From Figures 3b and 3c, both temperature and concentration profiles decreases with increasing values of *Gr*. The fluid temperature reduces at every point other than the plate and when the heated surface is in contact with the fluid, the result of temperature difference causes buoyancy force, which induces the natural convection [12].

Velocity, temperature and concentration profiles for different values of thermal radiation parameter with *Gr*=1.0, *γ*=0.5, *Sc*=0.2, *Q*=0.01, *Gm*=1.5, *Pr*=0.71, *M*=1.2 are displayed in Figures 4a, 4b and 4c. It was observed from Figure 4a that velocity profiles increased to a peak along the plate and gently decreases away towards the free stream with increasing values of thermal radiation parameter *N*.

It also revealed that increasing the values of *N* causes less interaction with the boundary layer. Figure 4b revealed that temperature profiles increases as thermal radiation parameter *N* increases. This was because thermal radiation in the fluid increases the temperature within the boundary layer which accelerates the convection as well as increases the flow within the boundary layer. In Figure 4c, concentration profiles decreased gradually along the plate towards the free stream as thermal radiation parameter increases.

For different values of the local magnetic field parameter *M*, the velocity profiles are plotted in Figure 5a. It was observed that velocity profiles decreases as *M* increases with tendency to resist the fluid flow. But the reverse was observed within the boundary layer for temperature and concentration profiles as shown in Figures 5b and 5c. It was observed that increasing local magnetic field parameter led to both increase in temperature of the fluid and concentration of the flow, which had an enhanced effect on the flow from the plate to the free stream [13].

Figure 6a presents the velocity profiles for various values of *Gm*. It was observed that increase in the values of *Gm*, have the tendency to induce more flow in the boundary layer due to the effect of thermal buoyancy, thereby producing an increase in velocity flow. Meanwhile, temperature and concentration profiles for *Gm* are presented in Figures 6b and 6c. It was observed that increasing the values of *Gm* with *Gr*=1.2, γ=0.5, *Sc*=0.22, *Q*=0.01, *N*=0.10, *Pr*=0.72, and *M*=2, both temperature and concentration profiles decrease gradually away from the free stream towards the vertical plate. Figures 7a–7b displayed the effects of *Sc* on the velocity, temperature and concentration profiles.

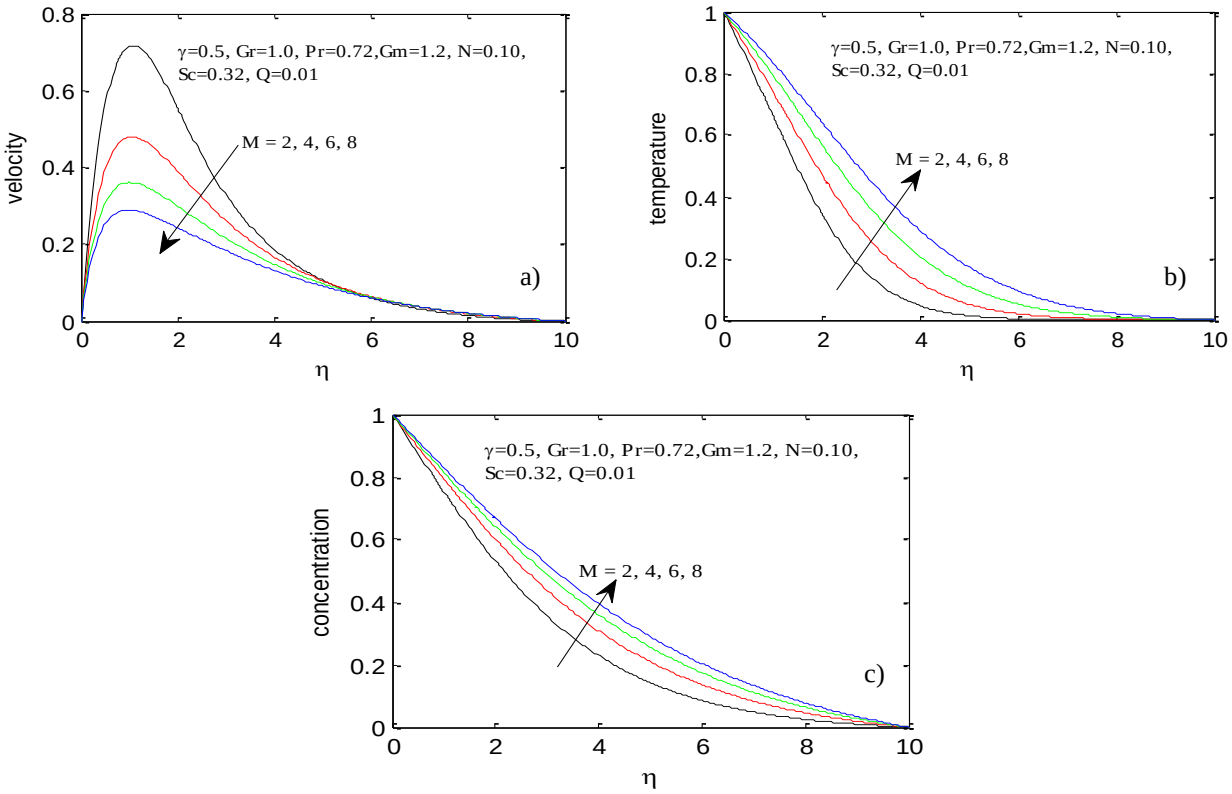

Figure 5. Variation of *f*'(η) (a), Temperature profiles θ(η) (b) and Variation of ϕ(η) (c) with η for Different Values of *M*

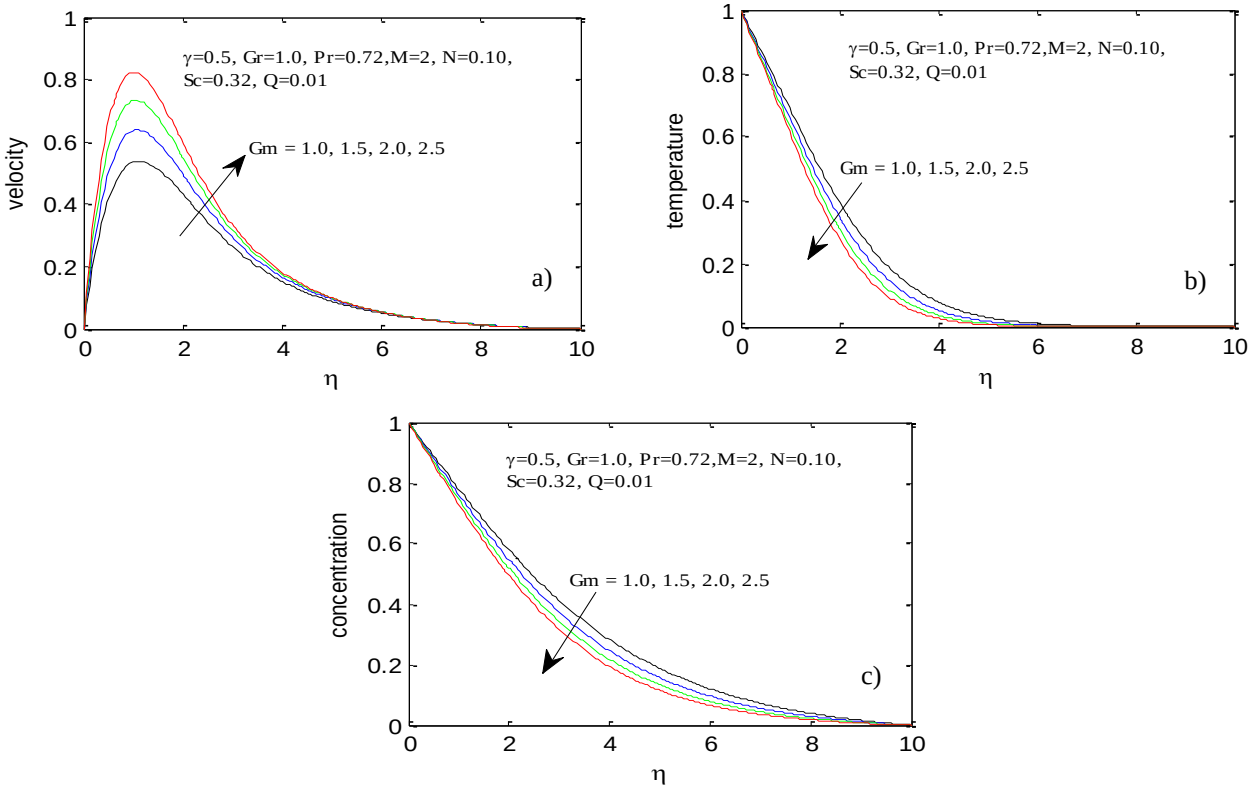

Figure 6. Velocity $f'(\eta)$ (a), Temperature $\theta(\eta)$ (b), Concentration $\phi(\eta)$ (c) Profiles for Different Values of Local Mass Grashof Number

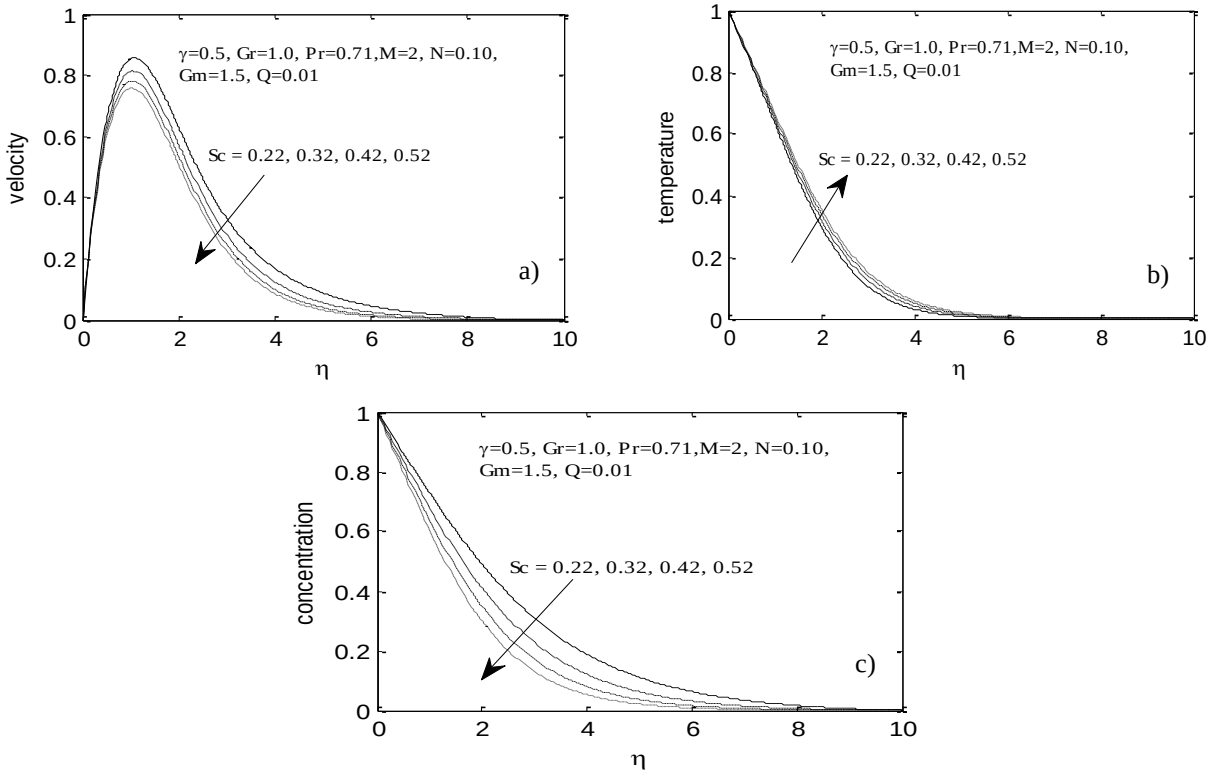

Figure 7. Velocity (a), Temperature (b) and Concentration (c) Profiles for Various Values of Schmidt Number *Sc*

From Figures 7a and 7c, it was observed that velocity and concentration profiles decreases respectively as *Sc* increases. Temperature profiles gradually increases away from the plate with increasing values of *Sc* towards the free stream region as shown in Figure 7b. The effects of local heat source parameter *Q* on the velocity, temperature and concentration profiles are displayed from Figures 8a–8c. From Figures 8a and 8b, it was observed that velocity and temperature profiles increases as

Q increases. While, from Figure 8c, concentration profiles decreases with increase in local heat generation parameter *Q*.

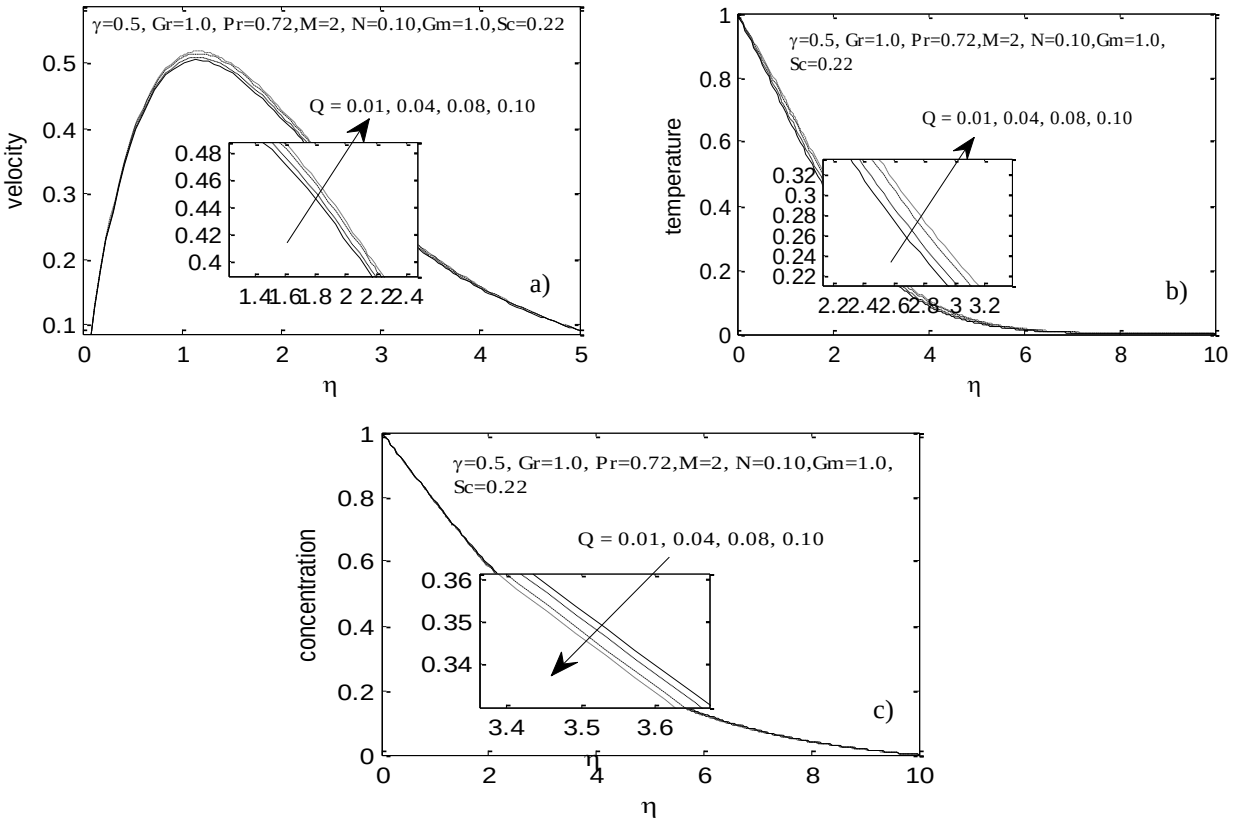

Figure 8. Velocity (a), Temperature (b) and Concentration (c) Profiles for Various Values of *Q*

However, it was observed that for various values of *Q*=0.01, 0.04, 0.08, 0.1 in Figures 8a–8c, little significant variations in the corresponding velocity, temperature and concentration profiles were noticed. The concentration boundary layer thickness reduces as a result of increase in the local heat source parameter thereby having significant effect on velocity and temperature distributions.

5. Conclusion

The problem resolving qualitative engineering problems via applied mathematical approach was considered. The solved coupled nonlinear ordinary differential equations and the effects of the various governing parameters on velocity, temperature and concentration profiles showed that the rate of heat transfer in terms of Nusselt number *Nu* decreases as *Pr*, *Gr*, ε and *Gm* decreases but with increasing values of *M*, γ, δ, *Ec*, *N*, *Q* and *Sc*.

ACKNOWLEDGEMENTS

I wish to acknowledge the support given to me to attend the FUOYE HUMBOLDT KOLLEG 2017 with all expenses paid by the AvH Foundation.

REFERENCES

[1] Harvard J.A., 2017. Paulson school of engineering and applied sciences, https://www.seas.harvard.edu/applied-mathematics

[2] www.Math.iit.edu (2017), Department of Applied Mathematics, Rattaliata Engineering Center, Chicago.

[3] Oyem O.A., 2016. Effects of thermo-physical properties on free convective heat and mass transfer flow over a vertical plate. *Ph.D Thesis*, Federal University of Technology Akure.

[4] Holman J.P., 2014. Heat transfer (9th edition), Tata McGraw-Hill Publishing Company Limited, New Delhi.

[5] Parvin S., Alim M.A., Hossain N.F., 2015. Heat and mass transfer due to double diffusive mixed convection in a parallel plate reactor in presence of chemical reaction and heat generation. Int. J. Chem. Proc. Eng. Res. 2(2), 17-29.

[6] Sandeep N., Sugunamma V.,2013. Effect of inclined magnetic field on unsteady free convective flow of dissipative fluid past a vertical plate. Open J. Adv. Eng. Tech., 1(1), 6-23.

[7] Siegel R., Howell J.R., 1992. Thermal radiation heat transfer (3rd edition). Hemisphere Publishing Corporation, Taylor and Francis Group, Washington.

[8] Mohyud-Din S.T., Yildirim A., Sezer S.A., Usman M., 2010. Modified variational iteration method for free-convective boundary-layer equation using Padé approximation. Math. Prob. Eng., 20(10), 1-11.

[9] Prasad K.V., Vajravelu K., Datti P.S., 2010. The effects of variable fluid properties on the hydromagnetic flow and heat transfer over a non-linearly stretching sheet. Int. J. Ther. Sci., 49, 603-610.

[10] Khaleque T.S., Samad M.A., 2010. Effects of radiation, heat generation and viscous dissipation on MHD free convection flow along a stretching sheet. Res. J. App. Sci. Eng. Tech., 2(4), 368-377.

[11] Jana R.N., Ghosh S.K., 2011. Radiative heat transfer of an optically thick gray gas in the presence of indirect natural convection. World J. Mech., 1, 64–69.

[12] Abah S.O., Eletta B.E., Omale, S.O., 2012. The numerical analysis of the effect of free convection heat and mass transfer on the unsteady boundary layer flow past a vertical plate. Int. J. Theo. Math. Phys., 2(3), 33-36.

[13] Shit G.C., Haldar R., 2012. Thermal radiation effects on MHD viscoelastic fluid flow over a stretching sheet with variable viscosity. Int. J. Appl. Math. Mech. 8(14), 14-36.

[14] Sobamowo M.G., 2017. On the explicit analytical solutions to large amplitude nonlinear oscillations arising structural engineering problems. ANNALS of Faculty of Engineering Hunedoara – Int. Journal of Engineering, Tome XV, Fascicule 3, 229-234.